Gyrotropic Magnetic Effect and the Magnetic Moment on the Fermi Surface

Shudan Zhong, Joel E. Moore, and Ivo Souza

Phys. Rev. Lett. **116**, 077201 — Published 18 February 2016

DOI: 10.1103/PhysRevLett.116.077201

Gyrotropic Magnetic Effect and the Magnetic Moment on the Fermi Surface

Shudan Zhong,[1] Joel E. Moore,[1,2] and Ivo Souza[3,4]

[1] *Department of Physics, University of California, Berkeley, CA 94720*
[2] *Materials Sciences Division, Lawrence Berkeley National Laboratory, Berkeley, CA 94720*
[3] *Centro de Física de Materiales, Universidad del País Vasco, 20018 San Sebastían, Spain*
[4] *Ikerbasque Foundation, 48013 Bilbao, Spain*

(Dated: January 19, 2016)

The current density $\boldsymbol{j}^{\mathbf{B}}$ induced in a clean metal by a magnetic field $\mathbf{B}$ is formulated as the low-frequency limit of natural optical activity, or natural gyrotropy. Working with a multiband Pauli Hamiltonian, we obtain from the Kubo formula a simple expression for $\alpha_{ij}^{\rm gme} = j_i^{\mathbf{B}}/B_j$ in terms of the intrinsic magnetic moment (orbital plus spin) of the Bloch electrons on the Fermi surface. An alternate semiclassical derivation provides an intuitive picture of the effect, and takes into account the influence of scattering processes in dirty metals. This "gyrotropic magnetic effect" is fundamentally different from the chiral magnetic effect driven by the chiral anomaly and governed by the Berry curvature on the Fermi surface, and the two effects are compared for a minimal model of a Weyl semimetal. Like the Berry curvature, the intrinsic magnetic moment should be regarded as a basic ingredient in the Fermi-liquid description of transport in broken-symmetry metals.

PACS numbers: 78.20.Ek,75.47.-m,71.18.+y

Introduction.— When a solid is placed in a static magnetic field the nature of the electronic ground state can change, leading to striking transport effects. A prime example is the integer quantum Hall effect in a quasi two-dimensional (2D) metal in a strong perpendicular field [1]. Novel magnetotransport effects have also been predicted to occur in 3D topological (Weyl) metals, such as an anomalous longitudinal magnetoresistence [2, 3], and the chiral magnetic effect (CME), where an electric pulse $\mathbf{E} \parallel \mathbf{B}$ induces a transient current $\boldsymbol{j} \parallel \mathbf{B}$ [4]; both are related to the chiral anomaly that was originally discussed for Weyl fermions in particle physics [5, 6]. In all these phenomena the role of the static $\mathbf{B}$-field is to modify the equilibrium state, but an $\mathbf{E}$-field is still required to put the electrons out of equilibrium and drive the current (since $\mathbf{E} = -\dot{\mathbf{A}}$, the vector potential is time-dependent even for a static $\mathbf{E}$-field).

Recently, the intriguing proposal was made that a pure $\mathbf{B}$-field could drive a dissipationless current in certain Weyl semimetals where isolated band touchings (the "Weyl points," or WPs) of opposite chirality are at different energies [7]. The existence of such an effect was later questioned [8], and the initial interpretation as an *equilibrium* current was discounted. (Indeed, that would a violate a "no-go theorem" attributed to Bloch that forbids macroscopic current in a bulk system in equilibrium [9].) Subsequent theoretical work suggests that the proposed effect can still occur in *transport*, as the current response to a $\mathbf{B}$-field oscillating at low frequencies [10–13].

At present the effect is still widely regarded as being related to the chiral anomaly [10] (or, more generally, to the Berry curvature of the Bloch bands [11–14]), and is broadly characterized as a type of "CME." We show in this Letter that the experimental implications and microscopic origin of this effect are both very different from the CME (as defined in Ref. [4], consistent with the particle-physics literature [15]). Experimentally, the effect is realized as the low-frequency limit of natural gyrotropy [16] in clean metals (see also Ref. 14), and we will call it the "gyrotropic magnetic effect" (GME). Both $\mathbf{E}$ and $\mathbf{B}$ optical fields drive the gyrotropic current, but at frequencies well below the threshold for interband absorption ($\hbar\omega \ll \epsilon_{\rm gap}$) their separate contributions can be indentified. This allows to infer from a low-frequency optical-rotation measurement the reactive current induced by the oscillating $\mathbf{B}$-field. The GME is predicted to occur not only in certain Weyl semimetals, but in any optically-active metal (a necessary but not sufficient condition is lack of an inversion center, and a sufficient but not necessary condition is structural chirality [17–19]).

Existing expressions for the natural gyrotropy current at low frequencies involve the Berry curvature of all the occupied states (and velocities of empty bands) [11–14], at odds with the notion that transport currents are carried by states near the Fermi level $\epsilon_{\rm F}$. Integrals over all occupied states involving the Berry curvature also appear in calculations of a part of the low-frequency optical activity [20–22], and of the intrinsic anomalous Hall effect (AHE); in the case of the AHE, a Fermi surface (FS) reformulation exists [23]. We find that the GME is not governed by the chiral anomaly or the Berry curvature, but by the intrinsic magnetic moment of the Bloch states on the FS. Our analysis also takes into account the finite relaxation time τ in real materials, which is shown to weaken the effect at the lowest frequencies. The magnitude of the GME in the clean limit $\omega\tau \gg 1$ is estimated for the optically-active semimetal $SrSi_2$ [24].

CME versus GME.— Both effects can be discussed by positing a linear relation between $\boldsymbol{j}$ and $\mathbf{B}$,

$$j_i = \alpha_{ij} B_j. \tag{1}$$

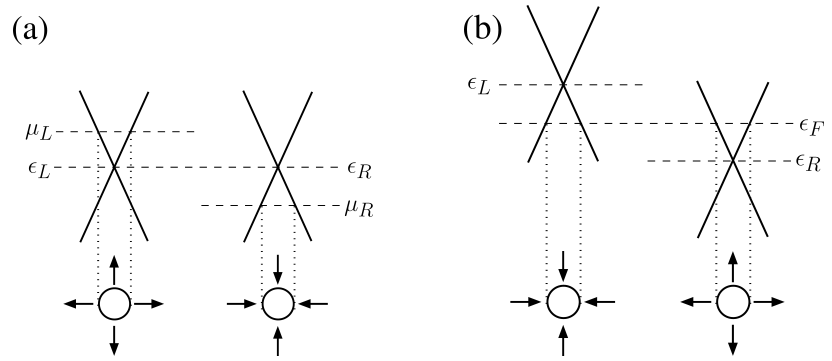

FIG. 1. (a) Chiral magnetic effect in a T-broken Weyl semimetal in a static $\mathbf{B}$-field. The left- and right-handed Weyl nodes are at the same energy $\epsilon_{\rm L} = \epsilon_{\rm R}$, but the enclosing Fermi pockets are not in chemical equilibrium ($\mu_{\rm L} \neq \mu_{\rm R}$) due to the application of an $\mathbf{E} \parallel \mathbf{B}$ pulse, and this drives the current [Eq. (3)]. (b) Gyrotropic magnetic effect. P symmetry is now broken along with T, leading to $\epsilon_{\rm L} \neq \epsilon_{\rm R}$. The Fermi pockets are in chemical equilibrium, $\mu_{\rm L} = \mu_{\rm R} = \epsilon_{\rm F}$, and an oscillating $\mathbf{B}$-field drives the current [Eq. (17)]. The bottom of each panel shows the Fermi pockets, and the arrows represent the Fermi velocities.

Suppose we use linear response to evaluate $\boldsymbol{\alpha}$ for a clean metal, describing the $\mathbf{B}$-field in terms of a vector potential that depends on both $\mathbf{q}$ and ω. The result will depend on the order in which the $\mathbf{q} \to 0$ and $\omega \to 0$ limits are taken [10–12], much as the compressibility and conductivity are different limits of electrical response. The CME tensor $\boldsymbol{\alpha}^{\rm cme}$ can be obtained from Eq. (1) in the equilibrium or *static* limit of the magnetic field (setting $\omega = 0$ before sending $\mathbf{q} \to 0$), with an additional step needed to describe the $\mathbf{E}$-field pulse. The GME tensor $\boldsymbol{\alpha}^{\rm gme}$ is extracted directly from Eq. (1) in the transport or *uniform* limit (sending $\mathbf{q} \to 0$ before $\omega \to 0$) that describes conductivities in experiment. (Here "$\omega \to 0$" means $\hbar\omega \ll \epsilon_{\rm gap}$, but note that $\omega\tau \gg 1$ because the clean limit $\tau \to \infty$ is assumed; effects caused by finite relaxation times in dirty samples will be discussed later.) Only $\boldsymbol{\alpha}^{\rm gme}$ is a material property, since the details of the $\mathbf{E}$-field pulse producing nonequilibrium are missing from $\boldsymbol{\alpha}^{\rm cme}$. Below we derive microscopic expressions for both.

Chiral magnetic effect.— The tensor $\boldsymbol{\alpha}$ calculated in the static limit is isotropic, $\alpha_{ij} = \alpha^{\rm stat}\delta_{ij}$, with

$$\alpha^{\rm stat} = -\frac{e^2}{\hbar}\sum_n \int [d\mathbf{k}]\, f^0_{\mathbf{k}n}\,(\mathbf{v}_{\mathbf{k}n}\cdot\boldsymbol{\Omega}_{\mathbf{k}n}) = 0\,, \qquad (2)$$

where $[d\mathbf{k}] = d^3k/(2\pi)^3$, the integral is over the Brillouin zone, $f^0_{\mathbf{k}n} = f(\epsilon_{\mathbf{k}n})$ is the equilibrium occupation factor, $\mathbf{v}_{\mathbf{k}n} = \boldsymbol{\partial}_{\hbar\mathbf{k}}\epsilon_{\mathbf{k}n}$ is the band velocity, $\boldsymbol{\Omega}_{\mathbf{k}n} = -{\rm Im}\langle\boldsymbol{\partial}_{\mathbf{k}}u_{\mathbf{k}n}| \times |\boldsymbol{\partial}_{\mathbf{k}}u_{\mathbf{k}n}\rangle$ is the Berry curvature, and $-e$ is the electron charge. Equation (2) was derived in Ref. [25] using the semiclassical formalism [26], and we obtain the same result from linear response [27]. The fact that $\alpha^{\rm stat}$ vanishes (see below) is in accord with Bloch's theorem [9].

To turn the above "quasiresponse" into $\alpha^{\rm cme}$, let us recast Eq. (2) as a FS integral. Integrating by parts produces two terms. The one containing $\boldsymbol{\partial}_{\mathbf{k}}\cdot\boldsymbol{\Omega}_{\mathbf{k}n}$ picks up monopole contributions from the occupied WPs, and vanishes because each WP appears twice with opposite signs [43]. In the remaining term we write $\boldsymbol{\partial}_{\mathbf{k}}f^0 = -\hat{\mathbf{v}}_{\rm F}\delta^3(\mathbf{k}-\mathbf{k}_{\rm F})$ with $\hat{\mathbf{v}}_{\rm F}$ the FS normal at $\mathbf{k}_{\rm F}$, and introduce the Chern number $C_{na} = (1/2\pi)\int_{S_{na}} dS\,(\hat{\mathbf{v}}_{\rm F}\cdot\boldsymbol{\Omega}_{\mathbf{k}n})$ of the a-th Fermi sheet S_{na} in band n [23, 43]. After assigning different chemical potentials to different sheets to account for the effect of the $\mathbf{E}$-field pulse Eq. (2) becomes $\alpha^{\rm cme} = -(e^2/h^2)\sum_{n,a}\mu_{na}C_{na}$, leading to the current density $\boldsymbol{j} = \alpha^{\rm cme}\mathbf{B}$ [4, 9]. In equilibrium $\mu_{na} = \epsilon_{\rm F}$, and using $\sum_{n,a}C_{na} = 0$ we find $\boldsymbol{j} = 0$, as per Eq. (2).

For a Weyl semimetal with two Fermi pockets with $C = +1$ and $C = -1$ placed at slightly different chemical potentials $\mu_{\rm L}$ and $\mu_{\rm R}$ [44] [Fig. 1(a)], a current develops,

$$\boldsymbol{j} = (e^2/h^2)\mathbf{B}(\mu_{\rm R} - \mu_{\rm L})\,. \qquad (3)$$

Gyrotropic magnetic effect.— Symmetry considerations already suggest a link between the GME and natural gyrotropy. Both $\boldsymbol{j}$ and $\mathbf{B}$ are odd under time reversal T, and $\boldsymbol{j}$ is odd under spatial inversion P while $\mathbf{B}$ is P-even, and so according to Eq. (1) the GME is T-even and P-odd, same as natural gyrotropy [16].

To make the connection precise, consider the current density induced by a monochromatic optical field $\mathbf{A}(t,\mathbf{r}) = \mathbf{A}(\omega,\mathbf{q})e^{i(\mathbf{q}\cdot\mathbf{r}-\omega t)}$ at first order in $\mathbf{q}$,

$$j_i(\omega,\mathbf{q}) = \Pi_{ijl}(\omega)A_j(\omega,\mathbf{q})q_l\,. \qquad (4)$$

The T-even part $\Pi^{\rm A}_{ijl}$ of the response tensor is antisymmetric under $i \leftrightarrow j$. It has nine independent components, and can be repackaged as a rank-2 tensor using [45, 46]

$$\Pi^{\rm A}_{ijl} = i\varepsilon_{ilp}\alpha^{\rm gme}_{jp} - i\varepsilon_{jlp}\alpha^{\rm gme}_{ip} \qquad (5a)$$

$$\alpha^{\rm gme}_{ij} = \frac{1}{4i}\varepsilon_{jlp}\left(\Pi^{\rm A}_{lpi} - 2\Pi^{\rm A}_{ilp}\right)\,. \qquad (5b)$$

At nonabsorbing frequencies $\boldsymbol{\alpha}^{\rm gme}(\omega)$ is real and $\boldsymbol{\Pi}^{\rm A}(\omega)$ is purely imaginary, but otherwise both are complex.

From now on we assume $\hbar\omega \ll \epsilon_{\rm gap}$, so that only intraband absorption can occur. In this regime $\boldsymbol{\alpha}^{\rm gme}$ satisfies

$$j_i^{\mathbf{B}} = -i\omega P_i^{\mathbf{B}} = \alpha_{ij}^{\rm gme} B_j \tag{6a}$$

$$M_i^{\mathbf{E}} = -(i/\omega)\alpha_{ji}^{\rm gme} E_j\,, \tag{6b}$$

where $\mathbf{E} = i\omega\mathbf{A}$ and $\mathbf{B} = i\mathbf{q}\times\mathbf{A}$, and $\mathbf{P}^{\mathbf{B}}$ and $\mathbf{M}^{\mathbf{E}}$ are oscillating moments induced by $\mathbf{B}$ and $\mathbf{E}$ respectively. The gyrotropic current $j_i^{\rm g} = \Pi^{\rm A}_{ijl}A_j q_l = j_i^{\mathbf{B}} + j_i^{\mathbf{E}}$ has contributions from both $\mathbf{B}$ and $\mathbf{E}$, with $\boldsymbol{j}^{\mathbf{B}}$ given by Eq. (6a) and $\boldsymbol{j}^{\mathbf{E}} = i\mathbf{q}\times\mathbf{M}^{\mathbf{E}}$. The dissipated power is $\mathrm{Re}(\boldsymbol{j}^{\rm g}\cdot\mathbf{E}^*)/2 = \omega\epsilon_{jlp}q_l \mathrm{Im}(\alpha_{ij}^{\rm gme})\mathrm{Re}(A_i^* A_p)$, confirming that $\mathrm{Re}\,\boldsymbol{\alpha}^{\rm gme}$ and $\mathrm{Im}\,\boldsymbol{\alpha}^{\rm gme}$ control the reactive and dissipative gyrotropic responses respectively.

In the long-wavelength limit Eq. (6a) describes a transport current induced by $\mathbf{B}$ in an optically-active metal (the *direct* GME), and Eq. (6b) describes a macroscopic magnetization induced by $\mathbf{E}$; the dc limit of this *inverse* GME has been previously discussed for metals with helical crystal structures [47].

To derive Eq. (6), consider a finite sample of size L. Using Eq. (20) of Ref. [46] for $\sigma^{\rm A}_{ijl} = (1/i\omega)\Pi^{\rm A}_{ijl}$ we find [48]

$$\alpha_{ij}^{\rm gme} = (\omega/2i)\left(\chi_{ij}^{\rm em} - \chi_{ji}^{\rm me}\right) + (\text{E. Q. terms})\,. \tag{7}$$

"E. Q." denotes electric quadrupole terms that keep $\boldsymbol{\alpha}^{\rm gme}$ origin-independent at higher frequencies [46, 49], but do not contribute to $\boldsymbol{j}^{\mathbf{B}}$ or $\mathbf{M}^{\mathbf{E}}$ when $\hbar\omega \ll \epsilon_{\rm gap}$, as they are higher-order in ω than the first term. The low-frequency gyrotropic response is controlled by the magnetoelectric susceptibilities $\chi_{ij}^{\rm em} = \partial P_i/\partial B_j$ and $\chi_{ij}^{\rm me} = \partial M_i/\partial E_j$. The dynamic polarization $P_i^{\mathbf{B}}$ can be decomposed into T-even and T-odd parts $(1/2)(\chi_{ij}^{\rm em} - \chi_{ji}^{\rm me})B_j$ and $(1/2)(\chi_{ij}^{\rm em} + \chi_{ji}^{\rm me})B_j$[50], and Eq. (6a) corresponds to the former. Similarly, Eq. (6b) gives the T-even part of the magnetization induced by $\mathbf{E}$. (The T-odd part of the magnetoelectric susceptibilities describes the linear magnetoelectric effect in insulators such as Cr_2O_3.)

In brief, the GME is the low-frequency limit of natural gyrotropy in P-broken metals, in much the same way that the AHE is the transport limit of Faraday rotation in T-broken metals. While the intrinsic AHE is governed by the geometric Berry curvature [23, 26] and becomes quantized by topology in Chern insulators, the GME is controlled by a nongeometric quantity, the intrinsic magnetic moment of the Bloch states [51].

To establish this result let us return to periodic crystals and derive a bulk formula for $\boldsymbol{\alpha}^{\rm gme}$ at $\hbar\omega \ll \epsilon_{\rm gap}$. From Kubo linear response in the uniform limit we obtain [27]

$$\Pi^{\rm A}_{ijl} = \frac{e^2\omega\tau}{1-i\omega\tau}\sum_n \int [d\mathbf{k}]\,\frac{\partial f}{\partial\epsilon_{\mathbf{k}n}}\Big[-\frac{g_s}{2m_e}\varepsilon_{ipl}v_{\mathbf{k}n,j}S_{\mathbf{k}n,p} + \frac{v_{\mathbf{k}n,i}}{\hbar}\mathrm{Im}\langle\partial_j u_{\mathbf{k}n}|H_{\mathbf{k}} - \epsilon_{\mathbf{k}n}|\partial_l u_{\mathbf{k}n}\rangle - (i\leftrightarrow j)\Big]. \tag{8}$$

(The calculation was carried out for a clean metal where formally $\tau = 1/\eta$ and $\eta \to 0^+$ [52]. Alternately one could retain a finite τ to give a phenomenological relaxation time in dirty metals, and indeed the semiclassical relaxation-time calculation to be presented shortly gives the same Drude-like dependence on $\omega\tau$ as Eq. (8).) $\mathbf{S}_{\mathbf{k}n}$ is the expectation value of the spin $\mathbf{S} = (\hbar/2)\boldsymbol{\sigma}$ of a Bloch state, $g_s \simeq 2$ is the spin g-factor of the electron, and m_e is the electron mass. Inserting Eq. (8) in Eq. (5b) gives

$$\alpha_{ij}^{\rm gme} = \frac{i\omega\tau e}{1-i\omega\tau}\sum_n\int [d\mathbf{k}]\,(\partial f/\partial\epsilon_{\mathbf{k}n})v_{\mathbf{k}n,i}m_{\mathbf{k}n,j}\,, \tag{9}$$

where $\mathbf{m}_{\mathbf{k}n} = -(eg_s/2m_e)\mathbf{S}_{\mathbf{k}n} + \mathbf{m}^{\rm orb}_{\mathbf{k}n}$ is the magnetic moment of a Bloch electron, whose orbital part is [26]

$$\mathbf{m}^{\rm orb}_{\mathbf{k}n} = \frac{e}{2\hbar}\mathrm{Im}\langle\boldsymbol{\partial}_{\mathbf{k}}u_{\mathbf{k}n}|\times(H_{\mathbf{k}} - \epsilon_{\mathbf{k}n})|\boldsymbol{\partial}_{\mathbf{k}}u_{\mathbf{k}n}\rangle\,. \tag{10}$$

At zero temperature, we can replace $\partial f/\partial\epsilon_{\mathbf{k}n}$ in Eq. (9) with $-\delta^3(\mathbf{k}-\mathbf{k}_{\rm F})/\hbar|\mathbf{v}_{\mathbf{k}n}|$ to obtain the FS formula

$$\alpha_{ij}^{\rm gme} = \frac{e}{(2\pi)^2 h}\frac{i\omega\tau}{i\omega\tau - 1}\sum_{n,a}\int_{S_{na}} dS\,\hat{v}_{{\rm F},i}m_{\mathbf{k}n,j}\,. \tag{11}$$

A nonzero $\mathbf{m}_{\mathbf{k}n}$ requires broken PT symmetry, but the GME can only occur if P is broken: with P symmetry present $\mathbf{m}_{-\mathbf{k},n} = \mathbf{m}_{\mathbf{k}n}$ and $\hat{\mathbf{v}}_{\rm F}(-\mathbf{k}_{\rm F}) = -\hat{\mathbf{v}}_{\rm F}(\mathbf{k}_{\rm F})$, leading to $\boldsymbol{\alpha}^{\rm gme} = 0$. Without spin-orbit coupling, only the orbital moment contributes.

Equations (6) and (11) are our main results. The GME is fully controlled by the bulk FS and vanishes trivially for insulators, contrary to the AHE where the FS formulation misses possible quantized contributions [23].

According to Eq. (11), the reactive response $\mathrm{Re}\,\boldsymbol{\alpha}^{\rm gme}$ is suppressed by scattering when $\omega \ll 1/\tau$. It increases with ω, and levels off for $\omega \gg 1/\tau$ (satisfying this condition without violating $\hbar\omega \ll \epsilon_{\rm gap}$ requires sufficiently clean samples). The opposite is true for the dissipative response $\mathrm{Im}\,\boldsymbol{\alpha}^{\rm gme}$, which drops to zero at $\omega \gg 1/\tau$ and becomes strongest at $\omega \ll 1/\tau$. In this lowest-frequency limit $\boldsymbol{j}^{\mathbf{B}} \to 0$, and Eqs. (6b) and (9) for the induced magnetization reduce to the expression in Ref. [47]. Thus, in the dc limit only a dissipative inverse GME occurs.

Semiclassical picture.— Our discussion of the GME assumed from the outset $\hbar\omega \ll \epsilon_{\rm gap}$. Since this is the regime where the semiclassical description of transport in metals holds [53], it is instructive to rederive Eqs. (6) and (11) by solving the Boltzmann equation. This provides an intuitive picture of the GME and its modification by scattering processes. The key ingredient beyond previous semiclassical approaches [20–22] is the correction to the band velocity (as opposed to the Berry-curvature anomalous velocity) in the presence of a magnetic field [26]: $\mathbf{v}_{\mathbf{k}n} = \boldsymbol{\partial}_{\hbar\mathbf{k}}\tilde{\epsilon}_{\mathbf{k}n}$, where $\tilde{\epsilon}_{\mathbf{k}n} = \epsilon_{\mathbf{k}n} - \mathbf{m}_{\mathbf{k}n}\cdot\mathbf{B}$.

In a static $\mathbf{B}$-field, the conduction electrons reach a new equilibrium state with $f^0_{\mathbf{k}n}(\mathbf{B}) = f(\tilde{\epsilon}_{\mathbf{k}n})$ as the distribution function [12], and the current vanishes according to Eq. (2). Under oscillating fields $\mathbf{E}$, $\mathbf{B} \propto e^{i(\mathbf{q}\cdot\mathbf{r}-\omega t)}$

the electrons are in an excited state with a distribution function $g_{\mathbf{k}n}(t,\mathbf{r})$ which we find by solving the Boltzmann equation in the relaxation-time approximation,

$$\partial_t g_{\mathbf{k}n} + \dot{\mathbf{r}}\frac{\partial g_{\mathbf{k}n}}{\partial \mathbf{r}} + \dot{\mathbf{k}}\frac{\partial g_{\mathbf{k}n}}{\partial \mathbf{k}} = -\left[g_{\mathbf{k}n} - f^0_{\mathbf{k}n}(\mathbf{B})\right]/\tau\,, \quad (12)$$

where τ is the relaxation time to return to the instantaneous equilibrium state described by $f^0_{\mathbf{k}n}(\mathbf{B}(t,\mathbf{r}))$ (for a slow spatial variation of $\mathbf{B}$). Using the semiclassical equations [26], the distribution function to linear order in $\mathbf{E}$ and $\mathbf{B}$ is $g_{\mathbf{k}n}(t,\mathbf{r}) = f^0_{\mathbf{k}n}(\mathbf{B}(t,\mathbf{r})) + f^1_{\mathbf{k}n}(t,\mathbf{r})$ with

$$f^1_{\mathbf{k}n} = \frac{\partial f/\partial\epsilon_{\mathbf{k}n}}{1 - \frac{\mathfrak{q}}{\omega}\cdot\mathbf{v}_{\mathbf{k}n} + \frac{i}{\omega\tau}}\left[\mathbf{m}_{\mathbf{k}n}\cdot\mathbf{B} + (ie/\omega)\mathbf{E}\cdot\mathbf{v}_{\mathbf{k}n}\right], \quad (13)$$

which at $\omega\tau \gg 1$ reduces to the result in Ref. 12.

As the current associated with $f^0_{\mathbf{k}n}(\mathbf{B})$ vanishes, the current induced by an oscillating $\mathbf{B}$-field is obtained by multiplying the first term in Eq. (13) with the band velocity. The result in the long-wavelength limit is

$$\boldsymbol{j}^{\mathbf{B}} = \frac{ie\omega\tau}{1-i\omega\tau}\sum_n \int [d\mathbf{k}]\,(\partial f/\partial\epsilon_{\mathbf{k}n})\,\mathbf{v}_{\mathbf{k}n}\,(\mathbf{m}_{\mathbf{k}n}\cdot\mathbf{B})\,, \quad (14)$$

in agreement with Eqs. (6a) and (9). Conversely, inserting the second term of Eq. (13) in the bulk expression for $\mathbf{M} = \mathbf{M}^{\rm spin} + \mathbf{M}^{\rm orb}$ [26] leads to Eqs. (6b) and (9) for the magnetization induced by an oscillating $\mathbf{E}$-field.

GME in two-band models.— Consider a situation where only two bands are close to $\epsilon_{\rm F}$, and couplings to more distant bands can be neglected when evaluating the orbital moment on the FS (for simplicity, we focus here on the orbital contribution to the GME in the clean limit). The 2×2 Hamiltonian written in the basis of the identity matrix and the three Pauli matrices is $H_{\mathbf{k}} = \bar{\epsilon}_{\mathbf{k}}\mathbb{1} + \mathbf{d}_{\mathbf{k}}\cdot\boldsymbol{\sigma}$, with eigenvalues $\epsilon_{\mathbf{k}t} = \bar{\epsilon}_{\mathbf{k}} + t d_{\mathbf{k}}$ where $t = \pm 1$ and $d_{\mathbf{k}} = |\mathbf{d}_{\mathbf{k}}|$. Equation (10) becomes

$$m^{\rm orb}_{\mathbf{k}t,i} = -\frac{e}{\hbar}\varepsilon_{ijl}\frac{1}{2d^2_{\mathbf{k}}}\mathbf{d}_{\mathbf{k}}\cdot(\partial_j\mathbf{d}_{\mathbf{k}}\times\partial_l\mathbf{d}_{\mathbf{k}})\,. \quad (15)$$

For orientation we study a minimal model for a Weyl semimetal where the FS consists of two pockets surrounding isotropic WPs of opposite chirality. We allow the WPs to be at different energies (this requires breaking P in addition to T), but $\epsilon_{\rm F}$ is assumed close to both [Fig. 1(b)]. Near each WP the Hamiltonian is $H_{\mathbf{k}\nu} = \epsilon_\nu\mathbb{1} + \chi_\nu\hbar v_{\rm F}\mathbf{k}\cdot\boldsymbol{\sigma}$, where ν labels the WP, ϵ_ν and $\chi_\nu = \pm 1$ are its energy and chirality (positive means right-handed), $\mathbf{k}$ is measured from the WP, and $v_{\rm F}$ is the Fermi velocity. From Eq. (15) $\mathbf{m}^{\rm orb}_{\mathbf{k}\nu} = -\chi_\nu(ev_{\rm F}/2k)\hat{\mathbf{k}}$, and only the trace piece $\overline{\alpha}^{\rm gme} = (\sum_i \alpha^{\rm gme}_{ii})/3$ survives is Eq. (11); in the clean limit each pocket contributes

$$\overline{\alpha}^{\rm gme}_\nu = \mp\frac{1}{3}\frac{e^2}{h^2}\chi_\nu\hbar v_{\rm F}k_{\rm F} = \frac{1}{3}\frac{e^2}{h^2}\chi_\nu(\epsilon_\nu - \epsilon_{\rm F})\,, \quad (16)$$

where the minus (plus) sign in the middle expression corresponds to $\epsilon_\nu < \epsilon_{\rm F}$ ($\epsilon_\nu > \epsilon_{\rm F}$). Summing over ν and using $\sum_\nu \chi_\nu = 0$ [54] gives $\overline{\alpha}^{\rm gme} = (e^2/3h^2)\sum_\nu \chi_\nu\epsilon_\nu$. For a minimal model $\nu = {\rm R}, {\rm L}$, and the GME current is

$$\boldsymbol{j}^{\mathbf{B}} = (e^2/3h^2)(\epsilon_{\rm R} - \epsilon_{\rm L})\mathbf{B}\,. \quad (17)$$

Equation (17) looks deceptively similar to Eq. (3) for the CME. The prefactor is different, but the key difference is in the meaning of the various quantities, and in their respective roles. To stress this point, we have in both equations placed the "force" that drives the current at the end, after the equilibrium parameter that enables the effect. The GME current is driven by the oscillating $\mathbf{B}$-field, while $\epsilon_{\rm L}$ and $\epsilon_{\rm R}$ are bandstructure parameters, with $\epsilon_{\rm R} - \epsilon_{\rm L}$ reflecting the degree of structural symmetry breaking that allows the effect to occur. Equation (3) is "universal" because of the topological nature of the FS integral involved, while Eq. (17) is for spherical pockets surrounding isotropic Weyl nodes. For generic two-band models [55], the non-FS expression found in Refs. [11, 12] for the orbital contribution to $\overline{\alpha}^{\rm gme}$ can be recovered from Eq. (9) in the clean limit [27].

We emphasize that breaking T is not required for the GME. If T is present (and P broken), the minimum number of WPs is four, not two [56]. In the class of T-symmetric Weyl materials so far discovered, T relates WPs of the same chirality and energy. Mirror symmetries connect WPs of opposite chirality so that $\boldsymbol{j}^{\mathbf{B}} = 0$, as expected since these symmetries tend to exclude optical activity [18, 19]. Fortuitously, the predicted Weyl material $SrSi_2$ has misaligned WPs of opposite chirality due to broken mirror symmetry [24]. Its optical activity coefficient ρ can be estimated from the energy splitting between WPs. Neglecting spin contributions that were not included in Eq. (17), each WP pair contributes [27]

$$\rho = (2\alpha/3hc)\,(\epsilon_{\rm L} - \epsilon_{\rm R})\,, \quad (18)$$

with α the fine-structure constant and c the speed of light. The calculated splitting $|\epsilon_{\rm L} - \epsilon_{\rm R}| \sim 0.1$ eV [24] gives $|\rho| \sim 0.4$ rad/mm per node pair, about the same as $|\rho| = 0.328$ rad/mm for quartz at $\lambda = 0.63$ μm [19]. This should be measurable in a frequency range from the infrared (above which the semiclassical assumptions break down) down to $1/\tau$, which depends on crystal quality. When $\epsilon_{\rm L} = \epsilon_{\rm R}$ the natural optical activity vanishes in equilibrium, but a nonequilibrium gyrotropic effect can still occur due to the chiral anomaly [21, 27].

In summary, we have elucidated the physical origin of currents induced by low-frequency magnetic fields in metals, in terms of the magnetic moment on the FS. Optical rotation measurements in the range $1/\tau \ll \omega \ll \epsilon_{\rm gap}/\hbar$ can be used to determine the reactive response ${\rm Re}\,\boldsymbol{\alpha}^{\rm gme}$. Unlike the CME [57] or the photoinduced AHE [58], no detailed model of nonequilibrium is required to quantify the GME, and efficient *ab initio* methods already exist to compute the needed orbital moments [59].

Note added: In another paper [60] submitted concurrently with the present one, the role of orbital moments in the natural gyrotropy of metals was also recognized.

We thank Q. Niu, J. Orenstein, D. Pesin, and D. Vanderbilt for useful comments, and also thank D. V. for calling our attention to Ref. [47] and suggesting a possible connection with the present work. We acknowledge support from grant NSF DMR-1507141 (S. Z.), from the DOE LBL Quantum Materials Program and Simons Foundation (J. E. M.), and from grants No. MAT2012-33720 from the Spanish government and No. CIG-303602 from the European Commission (I. S.).

[1] D. J. Thouless, M. Kohmoto, M. P. Nightingale, and M. den Nijs, Phys. Rev. Lett. **49**, 405 (1982).
[2] H. B. Nielsen and M. Ninomiya, Phys. Lett. **130B**, 389 (1983).
[3] D. T. Son and B. Z. Spivak, Phys. Rev. B **88**, 104412 (2013).
[4] D. T. Son and N. Yamamoto, Phys. Rev. Lett. **109**, 181602 (2012).
[5] S. Adler, Phys. Rev. **177**, 2426 (1969).
[6] J. S. Bell and R. Jackiw, Nuovo Cimento **60A**, 4 (1969).
[7] A. A. Zyuzin, S. Wu, and A. A. Burkov, Phys. Rev. B **85**, 165110 (2012).
[8] M. M. Vazifeh and M. Franz, Phys. Rev. Lett. **111**, 027201 (2013).
[9] N. Yamamoto, Phys. Rev. D **92**, 085011 (2015).
[10] Y. Chen, S. Wu, and A. A. Burkov, Phys. Rev. B **88**, 125105 (2013).
[11] P. Goswami and S. Tewari, arXiv:1311.1506 (2013).
[12] M.-C. Chang and M.-F.Yang, Phys. Rev. B **91**, 115203 (2015).
[13] M.-C. Chang and M.-F. Yang, Phys. Rev. B **92**, 205201 (2015).
[14] P. Goswami, G. Sharma, and S. Tewari, Phys. Rev. B **92**, 161110(R) (2015).
[15] D. E. Kharzeev, Prog. Part. Nucl. Phys. **75**, 133 (2014).
[16] The term *natural gyrotropy* refers to the time-reversal-even part of the optical response of a medium at linear order in the wavevector of light [17, 61]. The reactive part gives rise to natural optical activity, and the dissipative part to natural circular dichroism. Gyrotropic effects that are time-reversal-odd and zeroth order in the wavevector of light (e.g., Faraday rotation and magnetic circular dichroism [17]) are not considered in this work.
[17] L. D. Landau and E. M. Lifshitz, *Electrodynamics of Continuous Media*, 2nd ed. (Pergamon Press, Oxford, 1984).
[18] H. D. Flack, Helv. Chim. Acta **86**, 905 (2003).
[19] R. E. Newnham, *Properties of Materials* (Oxford University Press, Oxford, 2005).
[20] J. Orenstein and J. E. Moore, Phys. Rev. B **87**, 165110 (2013).
[21] P. Hosur and X.-L. Qi, Phys. Rev. B **91**, 081106 (2015).
[22] S. Zhong, J. Orenstein, and J. E. Moore, Phys. Rev. Lett. **115**, 117403 (2015).
[23] F. D. M. Haldane, Phys. Rev. Lett. **93**, 206602 (2004).
[24] S.-M. Huang, S.-Y. Xu, I. Belopolski, C.-C. Lee, G. Chang, B. Wang, N. Alidoust, M. Neupane, H. Zheng, D. Sanchez, A. Bansil, G. Bian, H. Lin, and M. Z. Hasan, arXiv:1503.05868 (2015).
[25] J.-H. Zhou, J. Hua, Q. Niu, and J.-R. Shi, Chin. Phys. Lett. **30**, 027101 (2013).
[26] D. Xiao, M.-C. Chang, and Q. Niu, Rev. Mod. Phys. **82**, 1959 (2010).
[27] See Supplemental Material [url], which includes Refs. [28-42].
[28] E. I. Blount, Solid State Physics **13**, 305 (1962).
[29] Y. Yafet, Solid State Physics **14**, 1 (1963).
[30] F. Wooten, *Optical Properties of Solids* (Academic Press, New York, 1972).
[31] M. Dressel and G. Grüner, *Electrodynamics of Solids* (Cambridge, 2002).
[32] W. A. Harrison, *Solid State Theory* (Dover, New York, 1980).
[33] W. Yao, D. Xiao, and Q. Niu, Phys. Rev. B **77**, 235406 (2008).
[34] K. Natori, J. Phys. Soc. Japan **39**, 1013 (1975).
[35] P. Hosur, A. Kapitulnik, S. A. Kivelson, J. Orenstein, and S. Raghu, Phys. Rev. B **87**, 115116 (2013).
[36] L. Barron, *Molecular Light Scattering and Optical Activity* (Cambridge University Press, Cambridge, 2004).
[37] B. Halperin, in *The Physics and Chemistry of Oxide Superconductors*, Springer Verlag Proceedings of Physics Vol 60, edited by Y. Iye and H. Yasuoka (Springer-Verlag, Berlin, 1992) p. 439.
[38] A. D. Fried, Phys. Rev. B **90**, 121112 (2014).
[39] V. M. Agranovich and V. I. Yudson, Opt. Commun. **9**, 58 (1973).
[40] V. V. Bokut and A. N. Serkyukov, Prikl. Spectrosk. **20**, 677 (1974).
[41] A. P. Vinogradov, Phys. Usp. **45**, 331 (2002).
[42] N. P. Armitage, Phys. Rev. B **90**, 035135 (2014).
[43] D. Gosálbez-Martínez, I. Souza, and D. Vanderbilt, Phys. Rev. B **92**, 085138 (2015).
[44] With our sign convention for the Berry curvature, a right-handed WP acts as a source in the lower band and as a sink in the upper band [26]. An enclosing pocket, either electron-like or hole-like, has Chern number $C = -1$.
[45] R. M. Hornreich and S. Shtrikman, Phys. Rev. **171**, 1065 (1968).
[46] A. Malashevich and I. Souza, Phys. Rev. B **82**, 245118 (2010).
[47] T. Yoda, T. Yokoyama, and S. Murakami, Sci. Rep. **5**, 12024 (2015).
[48] To recover the bulk result from Eq. (7), the $L \to \infty$ limit should be taken faster than the $\omega \to 0$ limit, consistent with the order of limits discussed earlier for transport.
[49] A. D. Buckingham and M. D. Dunn, J. Chem. Soc. A , 1988 (1971).
[50] This decomposition is obtained by invoking the Onsager relation $\chi^{\rm em}_{ij}(\omega)\big|_{-\mathbf{B}_{\rm ext}} = -\,\chi^{\rm me}_{ji}(\omega)\big|_{\mathbf{B}_{\rm ext}}$ [62].
[51] Here the term *geometric* refers to the intrisic geometry of the Bloch-state fiber bundle. The orbital moment of Bloch electrons can be considered geometric in a different sense: it is the imaginary part of a complex tensor whose real part gives the inverse effective mass tensor, i.e., the curvature of band dispersions [63].
[52] P. B. Allen, in *Conceptual foundations of materials properties: A standard model for calculation of ground- and excited-state properties*, Contemporary Concepts of Condens. Matt. Science, Vol. 1, edited by S. G. Louie and

M. L. Cohen (Elsevier, 2006) p. 165.
[53] N. W. Ashcroft and N. D. Mermin, *Solid State Physics* (Brooks Cole, 1976).
[54] H. Nielsen and M. Ninomiya, Nucl. Phys. **B185**, 20 (1981).
[55] In anisotropic models the traceless part of $\boldsymbol{\alpha}^{\mathrm{gme}}$ is generally nonzero. For any number of bands, it includes the traceless piece found previously [22], and the full tensor satisfies [27] the microscopic constraint from time-reversal invariance previously shown for one piece [22].
[56] S. M. Young, S. Zaheer, J. C. Y. Teo, C. L. Kane, E. J. Mele, and A. M. Rappe, Phys. Rev. Lett. **108**, 140405 (2012).
[57] S. A. Parameswaran, T. Grover, D. A. Abanin, D. A. Pesin, and A. Vishwanath, Phys. Rev. X **4**, 031035 (2014).
[58] K. F. Mak, K. L. McGill, J. Park, and P. L. McEuen, Science **344**, 1489 (2014).
[59] M. G. Lopez, D. Vanderbilt, T. Thonhauser, and I. Souza, Phys. Rev. B **85**, 014435 (2012).
[60] J. Ma and D. A. Pesin, Phys. Rev. B **92**, 235205 (2015).
[61] V. M. Agranovich and V. L. Ginzburg, *Crystal Optics with Spatial Dispersion, and Excitons*, 2nd ed. (Springer, Berlin, 1984).
[62] D. B. Melrose and R. C. McPhedran, *Electromagnetic Processes in Dispersive Media* (Cambridge University Press, Cambridge, 1991).
[63] Y. Gao, S. A. Yang, and Q. Niu, Phys. Rev. B **91**, 214405 (2015).